Journal of Catalysis 282 (2011) 209–214

Contents lists available at ScienceDirect

Journal of Catalysis

journal homepage: www.elsevier.com/locate/jcat

Aerobic oxidation of monoterpenic alcohols catalyzed by ruthenium hydroxide supported on silica-coated magnetic nanoparticles

Vinícius V. Costa [a], Marcos J. Jacinto [b], Liane M. Rossi [b], Richard Landers [c], Elena V. Gusevskaya [a,*]

[a] Departamento de Química, Universidade Federal de Minas Gerais, 31270-901 Belo Horizonte, MG, Brazil
[b] Instituto de Química, Universidade de São Paulo, 05508-000 São Paulo, SP, Brazil
[c] Instituto de Física, UNICAMP, 13083-970 Campinas, SP, Brazil

ARTICLE INFO

Article history:
Received 1 April 2011
Revised 13 June 2011
Accepted 14 June 2011
Available online 14 July 2011

Keywords:
Ruthenium
Magnetic catalysts
Oxidation
Oxygen
Monoterpenic alcohols

ABSTRACT

Ruthenium hydroxide supported on silica-coated magnetic nanoparticles was shown to be an efficient heterogeneous catalyst for the liquid-phase oxidation of a wide range of alcohols using molecular oxygen as a sole oxidant in the absence of co-catalysts or additives. The material was prepared through the loading of the amino modified support with ruthenium(III) ions from an aqueous solution of ruthenium(III) chloride followed by treatment with sodium hydroxide to form ruthenium hydroxide species. Characterizations suggest that ruthenium hydroxide is highly dispersed on the support surface, with no ruthenium containing crystalline phases being detected. Various carbonylic monoterpenoids important for fragrance and pharmaceutical industries can be obtained in good to excellent yields starting from biomass-based monoterpenic alcohols, such as isoborneol, perillyl alcohol, carveol, and citronellol. The catalyst undergoes no metal leaching and can be easily recovered by the application of an external magnet and re-used.

1. Introduction

The oxidation of alcohols is a fundamental organic transformation in both laboratory and industrial synthetic chemistry because the resulting carbonyl compounds are widely used in the preparation of pharmaceutical, agricultural, fragrance, and many others chemicals [1]. These reactions represent one of the most important challenges in green chemistry as many currently used processes still require stoichiometric amounts of expensive and/or toxic heavy metal oxidants producing, therefore, large amounts of wastes. Several homogeneous [2,3] and heterogeneous [4–9] transition metal catalysts were reported to promote the oxidation of alcohols with molecular oxygen as the final oxidant. These processes occur with high atom efficiency and give water as the only byproduct, which is especially relevant to environmental protection. In this field, solid materials containing ruthenium have attracted increasing attention because they can promote aerobic oxidations of a wide range of alcohols and do not require the presence of co-catalysts and/or additives such as bases or electron transfer mediators [10–24]. In particular, it has been reported the outstanding catalytic performance in these reactions of ruthenium hydroxide, $Ru(OH)_x$, supported on various solids, such as Al_2O_3 [10–12,20], TiO_2 [20–22], Fe_3O_4 [15], zeolites [23], and carbon nanotubes [24].

The development of new technologies for the separation and recycling of catalysts, especially those usually employed in liquid-phase batch processes, to substitute traditional time- and solvent-consuming procedures, e.g., extraction, filtration, and centrifugation, is another important goal for green chemistry. In this context, the use of magnetic materials as supports in heterogeneous catalysis has received a special attention because it provides a convenient route for the catalyst recovery by the application of an external permanent magnet [25–29]. Recently, we have developed magnetically recoverable cobalt and manganese catalysts for the liquid-phase oxidations of alkenes and thiols with molecular oxygen [30–32]. The catalysts were prepared through the incorporation of manganese or cobalt ions into framework positions of synthetic ferrites [30,31] or materials derived from iron-rich soils [32] and were stable to leaching. We have also prepared a core-shell magnetite-silica nanostructured support that provides enhanced stability to the magnetic core and new opportunities to be modified with different ligands, metals, or reactive moieties on the shell surface. Various catalysts have been prepared using the core-shell magnetic support, such as Rh [33], Pt [34], Pd [35], Au [36], and Ru [18]. The catalysts were synthesized by loading the support with the corresponding metal ions followed by metal reduction with hydrogen or $NaBH_4$. The ruthenium catalyst was found to be active in both Ru(III) (Fe_3O_4@SiO_2/Ru^{3+}) and Ru(0) (Fe_3O_4@SiO_2/Ru^0) forms for selective oxidation of model alcohols and hydrogenation of olefins, respectively [18]. In the present work, we have decided to incorporate ruthenium hydroxide on this

* Corresponding author. Fax: +55 31 34095700.
E-mail address: elena@ufmg.br (E.V. Gusevskaya).

0021-9517/$ - see front matter © 2011 Elsevier Inc. All rights reserved.
doi:10.1016/j.jcat.2011.06.014

magnetic support and tested the materials as catalysts in the aerobic oxidation of natural monoterpenic alcohols.

Terpenic compounds, in general, are an important biomass-based renewable feedstock for flavor and fragrance industries [37]. For several years, we have been interested in catalytic transformations of natural products, including terpenes, to more valuable chemicals, in particular, via aerobic oxidations over cobalt [30,31,38] and palladium [39–42] catalysts. In continuation of our ongoing project aimed at adding value to natural ingredients of essential oils, we report herein the ruthenium catalyzed oxidation of various monoterpenic alcohols with molecular oxygen to give valuable fragrance aldehydes and ketones. In order to improve catalyst separation, a core-shell silica-coated magnetic support was used for the immobilization of ruthenium hydroxide. The material was found to be an efficient heterogeneous catalyst for these reactions acting in the absence of any co-catalysts or additives. The magnetic properties of the catalyst allow for its facile separation from the reaction medium by means of an external magnetic field.

2. Experimental

2.1. Support preparation

The core-shell magnetite@silica support was prepared as reported in our previous works [18,33]. In a typical experiment, 44.6 g of Polyoxyethylene(5) isooctylphenyl ether was dispersed in 700 mL of cyclohexane. Then, 200 mg Fe_3O_4 (dispersed in cyclohexane) was added. The mixture was stirred until it became transparent. After this step, 9.44 mL of ammonium hydroxide (29%) was added to form a reverse microemulsion. Finally, 7.70 mL of tetraethylorthosilicate (TEOS) was added. The solution was gently stirred for 16 h. The core-shell nanocomposite Fe_3O_4@SiO_2 was precipitated with methanol and collected by centrifugation at 7000 rpm. After being washed with ethanol, the collected material was dried in vacuum, resulting in ca. 1 g of material. Then, the solid was modified with amino groups by reaction with 3-aminopropyltriethoxysilane (APTES) in dry toluene under N_2. The amine-functionalized solid (Fe_3O_4@SiO_2–NH_2) was washed with toluene, separated by centrifugation, and dried at 100 °C for 20 h.

2.2. Catalyst preparation

For the catalyst preparation, 500 mg of the material Fe_3O_4@SiO_2–NH_2 was added to 20 mL of an aqueous solution of $RuCl_3$ (0.75 mg mL^{-1}). The solution was stirred for 2 h at room temperature, and then the solid was magnetically isolated and washed with ethanol and acetone. After drying under vacuum for 10 min, the magnetic solid containing Ru^{3+}, Fe_3O_4@SiO_2/Ru^{3+}, was redispersed in 20 mL of water and kept under stirring for 10 min. The conversion of Ru^{3+} to $Ru(OH)_x$ was carried out by adding NaOH (0.1 M) until the pH was stable at 10. The resulting solution was stirred for 2 h, separated magnetically and dried with ethanol and ketone. The material dubbed Fe_3O_4@SiO_2/$Ru(OH)_x$ contains 1.4 wt.% Ru as characterized ICP-AES.

2.3. Catalyst and support characterization

2.3.1. Chemical analysis

The ruthenium content in the solid catalyst was measured using an inductively coupled plasma optical emission spectrometer ICP-OES Genisis SOP (Spectro). Reference solutions of Ru (1000 mg L^{-1}) with a high degree of analytical purity (ICP Standard, SpecSol) were used to obtain the calibration curves. Deionized water (MILLI-Q) was used to prepare all solutions. The sample digestion was carried out at 100 °C for 3 h with 5 mL aqua regia. The volume of the samples was then adjusted to 25 mL using DI water. The Ru content was quantified in duplicate for each sample.

2.3.2. X-ray photoelectron spectroscopy (XPS)

The X-ray photoelectron spectra were obtained with a VSW HA-100 spherical analyzer using an aluminum anode (AlKα line, $h\nu$ = 1486.6 eV) X-ray source. The high-resolution spectra were measured with constant analyzer pass energies of 44 eV, which produce a full width at half-maximum (FWHM) line width of 1.7 eV for the Au ($4f_{7/2}$) line. The powdered samples were pressed into pellets and fixed to a stainless steel sample holder with double-faced tape and analyzed without further preparation. To correct for charging effects, the spectra were shifted so that the Si(2p) binding energy of SiO_2 was 103.5 eV. Curve fitting was performed using Gaussian line shapes, and a Shirley type background was subtracted from the data.

2.3.3. X-ray diffraction (XRD)

The XRD experiments were carried out on a Rigaku-Denki powder diffractometer equipped with a curved graphite crystal using Cu Kα radiation λ = 1.5418 Å. The diffraction data were collected at room temperature in a Bragg–Brentano θ–2θ geometry with scan range between 10° and 100° with constant step $\Delta 2\theta$ = 0.02.

2.3.4. Transmission Electron Microscopy (TEM)

The TEM experiments were carried out on a Philips CM 200 operating at accelerating voltage of 200 kV. The samples for TEM were prepared by placing a drop of the nanoparticles solution on a carbon-coated copper grid.

2.4. Catalytic oxidation experiments

The reactions were carried out in a stainless steel reactor equipped with a magnetic stirrer. In a typical run, a mixture of the substrate (1.0 mmol), toluene (5 mL), and the catalyst (0.02–0.2 g; ca. 0.45–4.5 wt.%; Ru: 0.28–2.80 mol%) was transferred in the reactor. The reactor was pressurized with oxygen to the total pressure of 10 atm and placed in an oil bath; then, the solution was intensively stirred at 80–120 °C for the reported time. The reactions were followed by gas chromatography (GC) (Shimadzu 17 instrument, Carbowax 20 M capillary column). To take the aliquots for the GC analysis at appropriate time intervals, stirring was stopped and the catalyst was quickly settled by the application of an external permanent magnet. The structures of the products were confirmed by GC/MS (Shimadzu QP2010-PLUS instrument, 70 eV).

Catalyst recycling experiments were performed as follows: after the reaction, the catalyst was magnetically fixed at the bottom of the reactor, then the solution was taken off with a pipette, and the reactor was recharged with the fresh substrate. To control metal leaching, the catalyst was removed at the reaction temperature after the reaction was completed; the solution was recharged with the fresh substrate and allowed to react further.

3. Results and discussion

3.1. Characterization of the catalysts

The catalyst Fe_3O_4@SiO_2/$Ru(OH)_x$ was prepared in two steps, first the magnetic solid, previously modified with APTES, was submitted to a $RuCl_3$ aqueous solution, and then the isolated magnetic solid loaded with Ru^{3+} ions was treated with NaOH until pH 10 to prepare ruthenium hydroxide species. The content of Ru in the solid was 1.4 wt.% as determined by ICP-OES analyses. TEM images of

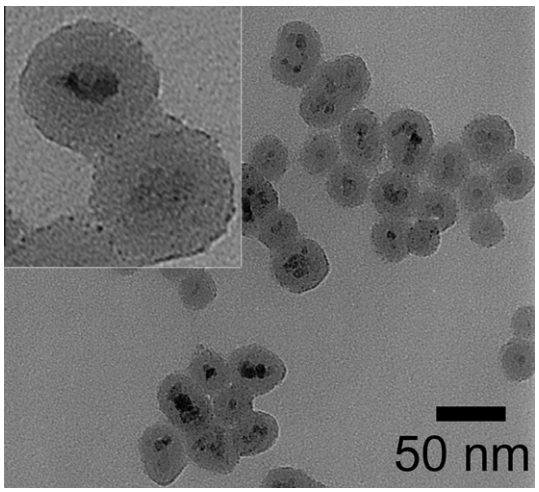

Fig. 1. TEM micrographs of the ruthenium catalyst Fe_3O_4@SiO_2/$Ru(OH)_x$ as prepared.

Fe_3O_4@SiO_2/$Ru(OH)_x$ displayed the core-shell morphology typical of the catalyst support presented in our previous work [33,34], but nanoparticles of ruthenium metal or ruthenium hydroxide could not be easily distinguished from the catalyst support using conventional TEM (Fig. 1). Enlarged TEM micrographs such as the presented in the inset of Fig. 1 do not revealed metal particles larger than 1–2 nm on the catalyst support surface. The magnetic support Fe_3O_4@SiO_2–NH_2 exhibits a core-shell morphology formed by Fe_3O_4 nanoparticles (ca. 10 nm) spherically coated with a layer of dense silica and the BET surface area of 62 $m^2\ g^{-1}$. The Fe_3O_4 @SiO_2 spheres reach the average size of ca. 40 nm and exhibit superparamagnetism in a large range of temperature with very high saturation magnetization M_S at room temperature, as reported previously [18]. The XRD pattern for Fe_3O_4@SiO_2/$Ru(OH)_x$ shows the Bragg diffractions characteristic of the Fe_3O_4 phase and of amorphous silica at $2\theta = 23°$. No diffraction peaks that could be attributed to ruthenium phases were observed, probably due to the low loading of ruthenium compared with Fe_3O_4 (ca. 9 wt.%) and the high dispersion of ruthenium on the support surface, as observed by TEM analysis.

The surface analysis by XPS was used to clarify the chemical states of surface ruthenium species. Fig. 2a and b show the Ru 3d and Ru 3p spectra of the ruthenium catalyst. The binding energy of the Ru 3d level was found in the range characteristic of Ru^{3+}/Ru^{4+} species, although the overlapping of signals for both species and the C 1s makes unequivocal determination difficult. The C ls emission at 285.4 eV interferes mostly with the $3d_{3/2}$ component, but the deconvoluted spectrum shows two doublets that can be attributed to two chemically different ruthenium entities with peak binding energies of 280.4 and 282.6 eV (Ru $3d_{5/2}$), and 284.5 and 286.7 eV (Ru $3d_{3/2}$). The peak positions confirm the presence of two distinct electron-deficient ruthenium species ($Ru^{\sigma+}$), since these values are slightly higher than the characteristic value of Ru(0), expected at 279.9–280.3 eV [43,44]. In both cases, the Ru $3d_{5/2}$ and Ru $3d_{3/2}$ peaks can be identified by taking into account the spin orbit splitting of ca. 4.1 eV for Ru $3d_{5/2}$ and Ru $3d_{3/2}$ and the expected intensity ratio of $I_{3/2}/I_{5/2} \approx 0.66$. The binding energy of the Ru 3p level can also be analyzed to provide a better distinction between ruthenium species. Yamaguchi et al have recently reported the XPS spectrum of a pristine sample of $Ru(OH)_x$ prepared by treating $RuCl_3$ with NaOH and used the binding energies of Ru $3p_{3/2}$ and Ru $3p_{1/2}$ core level at 462.9 and 484.8 eV, respectively, to confirm the average oxidation state of the ruthenium species as Ru^{3+} [45]. In Fig. 1b, the Ru $3p_{3/2}$ signal could be deconvoluted

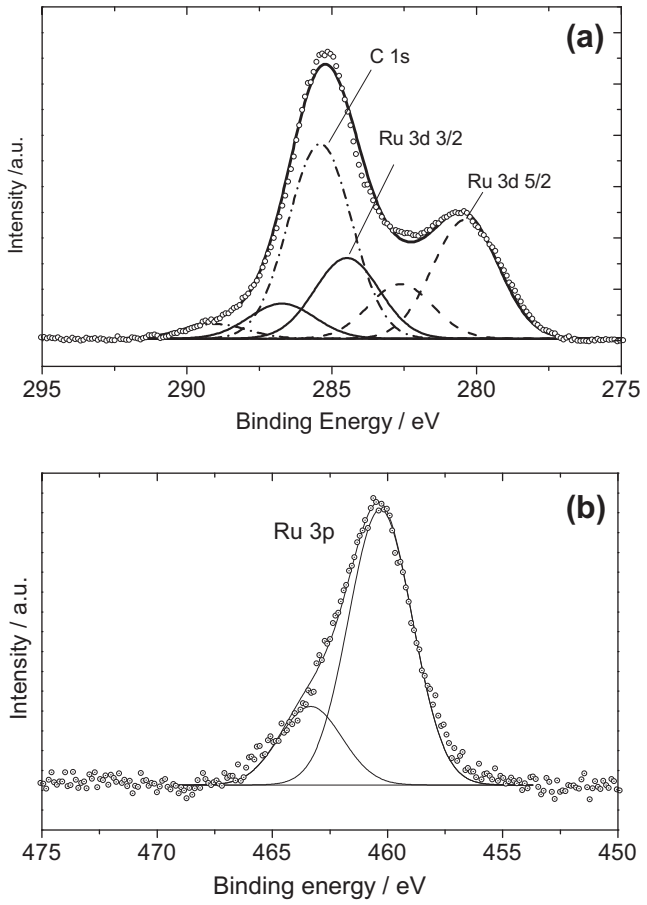

Fig. 2. (a) High-resolution Ru 3d XPS spectrum and its simulated peak fitting in the region of 275–295 eV, (b) high-resolution Ru 3p XPS spectrum and its simulated peak fitting in the region of 470–450 eV of the ruthenium catalyst (Fe_3O_4@SiO_2/$Ru(OH)_x$).

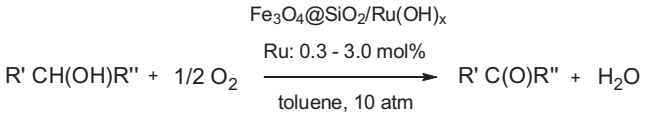

Scheme 1. Oxidation of alcohols into corresponding aldehydes or ketones.

into two peaks at 462.2 and 464.2 eV that can also be attributed to two chemically different oxidized ruthenium entities, consistent with the 3d deconvolution. Due to the large line width of the 3p lines, these values are only indicative. The oxygen O 1s signal could be deconvoluted into two peaks at 530.95 and 533.6 eV. The last one is the most intense and refers to SiO_2 (catalyst support) and the first one can be attributed to Ru–OH species, according to the literature [46].

3.2. Catalytic studies

The catalytic activity of the Fe_3O_4@SiO_2/$Ru(OH)_x$ material in the oxidation of alcohols was examined in toluene solutions under the atmosphere of molecular oxygen. A wide variety of primary and secondary alcohols was used as substrates including sterically hindered cyclic alcohols. In all experiments, this material was applied as a sole catalyst in the absence of any co-catalysts or additives. Corresponding aldehyde and ketones were detected as major, often exclusive, products of these reactions (Scheme 1). Representative results are collected in Table 1.

Table 1
Ru-catalyzed oxidation of alcohols in toluene solutions[a].

Run	Substrate	Catalyst (mg/mol% Ru)	Temperature (°C)	Time (h)	Conversion (%)	Product	Selectivity (%)	TON[b]
1	Benzyl alcohol (**1a**)	20/0.28	80	5	98	**1b**	100	350
2[c]	Benzyl alcohol (**1a**)	20/0.28	80	5	95	**1b**	100	700
3[d]	Benzyl alcohol (**1a**)		80	5	<3%			
4	1-Phenylpropanol (**2a**)	30/0.42	80	7	98	**2b**	100	233
5	Nerol (**3a**)	40/0.56	80	4	50	**3b**	75	90
6	Perillyl alcohol (**4a**)	130/1.82	100	5	98	**4b**	97	
7	Isoborneol (**5a**)	40/0.56	100	10	95	**5b**	100	175
8	Carveol (**6a**)	200/2.80	120	6	97	**6b**	95	35
9	Menthol (**7a**)	200/2.80	120	7	17	**7b**	100	
10	Isopulegol (**8a**)	200/2.80	120	7	11	**8b**	100	6
11	Citronellol (**9a**)	200/2.80	100	9	60	**9b**	88	3

[a] Conditions: substrate (1.0 mmol); Fe_3O_4@SiO_2/Ru(OH)$_x$ catalyst (1.4 wt.% Ru); toluene (5.0 mL); 10 atm (O_2). Conversion and selectivity were determined by GC.
[b] TON – moles of the substrate converted/moles of Ru. TON was calculated with respect to the total amount of ruthenium.
[c] The catalyst was re-used after run 1; total TON is given for two reaction cycles (runs 1 and 2).
[d] After run 2, the catalyst was removed, the solution was recharged with the fresh substrate (1 mmol), and the reaction was allowed to proceed further.

First of all, we studied the behavior of the prepared catalyst in the oxidation of benzylic alcohols, which were chosen as test reactants. The oxidation of benzyl alcohol (**1a**) with molecular oxygen occurred smoothly over the Fe_3O_4@SiO_2/Ru(OH)$_x$ material (Table 1, run 1), whereas in the presence of the support particles, Fe_3O_4@SiO_2–NH_2, or without any catalyst added the conversion of benzyl alcohol was negligible. The reaction gave benzaldehyde (**1b**) in a quantitative yield with not even trace amounts of benzoic acid being detected in the reaction solutions (Scheme 2). A virtually complete conversion was achieved for 5 h at 80 °C with the average turnover frequency (TOF) of nearly 70 min^{-1}.

The reaction with benzyl alcohol occurred with low catalyst loadings (0.45 wt.%, 0.28 mol% of Ru) resulting, therefore, in high turnover number (TON) of ca. 350. This result reflects the high stability of the catalyst and puts it among the most efficient catalysts reported so far in terms of TONs [10,16,20]. It is also important that the catalyst is a solid material that is insoluble in the reaction mixture and can be separated from the products magnetically. The results of the next run (run 2, Table 1) confirmed that the catalyst can be re-used after the removal of the supernatant solution without any further specific treatment or washing. After run 1, the catalyst was magnetically fixed at the bottom of the reactor, the solution was taken off with a syringe, and the reactor was recharged with the fresh solvent and substrate. A behavior of the spent catalyst with the fresh substrate was nearly the same as that in the original reaction (Table 1, cf. runs 1 and 2). The results of these runs correspond to the TON of nearly 700 with respect to the total amounts of ruthenium in the material. However, the real efficiency of the surface ruthenium atoms is much higher, because not all ruthenium atoms are accessible for the substrate, obviously. Magnetic properties of the catalysts allowed the easy and rapid procedure for its recovering and re-using to avoid conventional time-consuming techniques such as centrifugation, decantation, or filtration. The morphology of the spent catalyst isolated after two successive oxidation reactions (after the reaction shown in run 2, Table 1) was assessed from analysis of TEM micrographs such as the one presented in Fig. 3. It can be seen that the core-shell morphology of the catalyst support did not changed after exposition to reaction conditions and the magnetic material was preserved. Although the dispersion of ruthenium on the support surface is not as good as in the case of the fresh catalyst (Fig. 1), there is no evidence of the coalescence or formation of large metal particles.

To control leaching of the active metal, the catalyst after run 2 was removed; the transparent solution was recharged with the fresh substrate and allowed to react further (Table 1, run 3). Practically no conversion of benzyl alcohol was observed after catalyst removing; thus, the reaction was completely stopped in the absence of the catalyst. This result supports heterogeneous catalysis, i.e., the reaction solution contains no significant amounts of

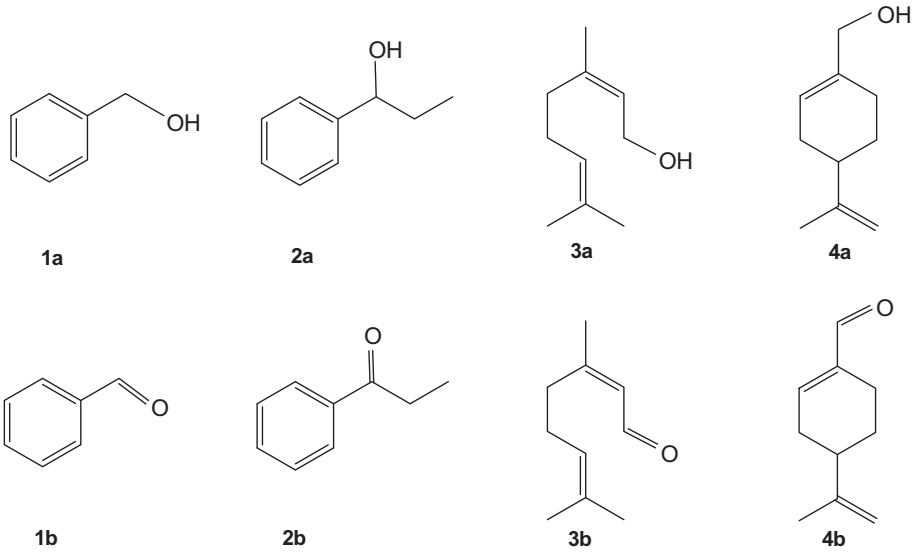

Scheme 2. Structures of alcoholic substrates **1a**–**4a** and corresponding products **1b**–**4b**.

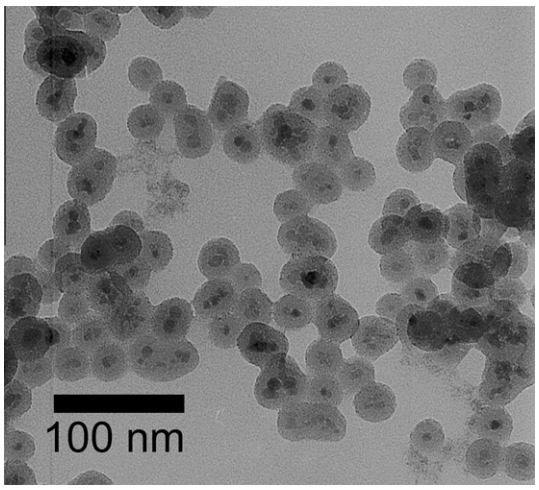

Fig. 3. TEM micrograph of the spent ruthenium catalyst Fe_3O_4@SiO_2/Ru(OH)$_x$ after two successive reactions of the oxidation of benzyl alcohol.

dissolved ruthenium species so that ruthenium ions immobilized in the solid matrix are responsible for the substrate oxidation. Thus, the catalyst releases no ruthenium to the medium and can be easily recovered either by magnetically or by centrifugation and re-used.

A secondary benzylic alcohol, 1-phenylpropanol (**2a**), can also be oxidized under similar conditions to give corresponding ketone **2b** (Scheme 2) in a nearly quantitative yield (Table 1, run 4). The reaction with this substrate was slower than that with benzyl alcohol; therefore, larger amounts of the catalyst and longer reaction time were needed to achieve a complete conversion at the same temperature (80 °C) (Table 1, cf. runs 1 and 4).

In a further work, we have tested in this reaction various natural monoterpenoid alcohols aiming, on the one hand, to clarify the substrate scope and, on the other hand, to synthesize carbonylic terpenoids, which can be useful for fragrance and pharmaceutical industries. With most of the alcohols, several experiments were performed at different temperatures and with different catalyst amounts in the attempt to obtain better yields for corresponding aldehydes or ketones. The results of the reactions that have shown the best yields are presented in Table 1.

Nerol (**3a**), a monoterpenic primary allylic alcohol available from many essential oils, was readily oxidized over the Fe_3O_4@SiO_2/Ru(OH)$_x$ catalyst giving as a major product (*Z*)-citral (**3b**), an important aroma compound with a strong lemon odor (Table 1, run 5; Scheme 2). Unfortunately, citral is not stable under the applied conditions, which has been shown by a control experiment using citral as the substrate. Citral was gradually consumed giving a mixture of unidentified products, some of them being not GC detectable. Probably for this reason, selectivity for citral at the oxidation of nerol drops with the reaction time from 90% at 25% conversion to 30% at 90% conversion (not shown in Table 1). In run 5, citral was obtained with 75% selectivity at 50% conversion of the substrate.

On the other hand, the oxidation of another monoterpenic primary allylic alcohol, perillyl alcohol (**4a**), occurred with an excellent selectivity giving almost quantitatively perillyl aldehyde (**4b**) (Scheme 2; Table 1, run 6). Perillyl aldehyde is a highly valuable compound used as food additive for flavoring and in perfumery to add spiciness, being much more expensive than original alcohol **4a**. It is important to note that no formation of corresponding carboxylic acids, even in trace amounts, has been detected during the oxidation of primary alcohols **1a**, **3a**, and **4a** in the presence of Fe_3O_4@SiO_2/Ru(OH)$_x$, reflecting high selectivity of this catalyst.

The Fe_3O_4@SiO_2/Ru(OH)$_x$ material is also very effective catalyst for the oxidation of sterically hindered isoborneol (**5a**) giving almost quantitatively camphor (**5b**) (Scheme 3), a compound with a strong, aromatic odor used as a local analgesic, respiratory stimulant, plasticizer, and an antimicrobial agent (Table 1, run 7). Isoborneol, a monoterpenic bicyclic secondary alcohol, is found in several plants, but mostly it is produced synthetically by the hydration of camphene [47].

The oxidation of the commercial (Sigma–Aldrich) mixture of *trans* and *cis* isomers of carveol (**6a**) over Fe_3O_4@SiO_2/Ru(OH)$_x$ gave carvone (**6b**) with 95% selectivity at nearly complete conversion (Scheme 3, Table 1, run 8). Carveol is a monoterpenic allylic alcohol with a *para*-menthenic skeleton, likewise perillyl alcohol **4a**; however, it is a secondary alcohol. The steric hindrance of the hydroxyl group resulted in lower reactivity of carveol as compared to perillyl alcohol as a similar reaction rate was attained at higher temperature and higher catalyst loading (Table 1, cf. runs 8 and 6). Thus, the catalyst can be used for the selective transformation of α,β-unsaturated alcohols into corresponding α,β-unsaturated aldehydes or ketones without intramolecular hydrogen transfer and isomerization.

Non-activated *para*-menthenic alcohols, menthol (**7a**), and isopulegol (**8a**), both cyclic secondary alcohols (Scheme 3), were shown

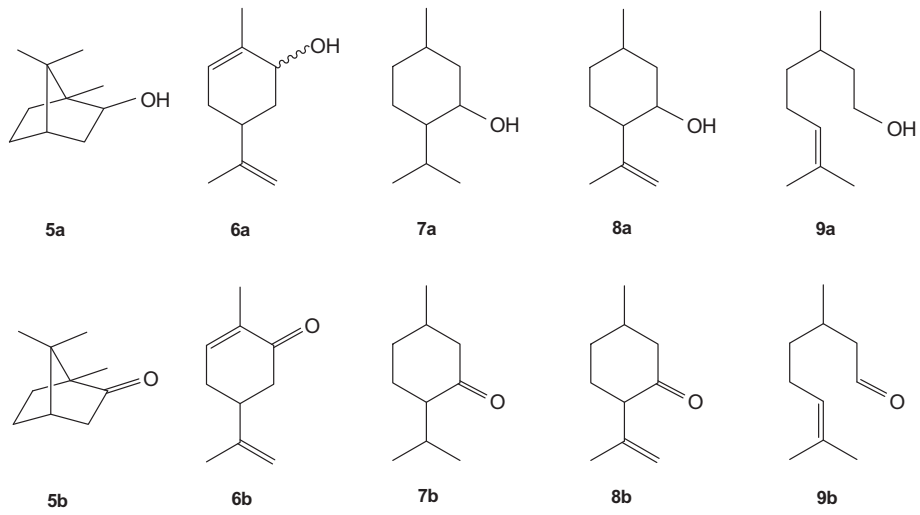

Scheme 3. Structures of alcoholic substrates **5a**–**9a** and corresponding products **5b**–**9b**.

to be much more resistant to oxidation under similar conditions than carveol. Although the reactions were highly selective to corresponding ketones (menthone **7b** and isopulegone **8b**, both used in perfumery and cosmetics for their characteristic aromatic odors), less than 20% conversions were attained in 7-h reactions at 120 °C (Table 1, runs 9 and 10).

Finally, we have tested the reactivity of citronellol (**9a**), a non-activated acyclic primary alcohol (Scheme 3). The reaction occurred at a reasonable rate at 100 °C giving citronellal (**9b**) in ca. 90% selectivity at 60% conversion (Table 1, run 11). However, at higher conversions selectivity decreased, probably, due to the concomitant transformations of the primarily formed citronellal.

The results obtained in the present work are in agreement with the mechanism generally accepted for the catalysts based on ruthenium hydroxide [15,20]. The faster oxidation of the primary alcohol **1a** as compared to the secondary alcohol **2a** suggests that the first step of the reaction is the formation of Ru–alkoxide species through the ligand exchange between an alcohol and a surface OH moiety. Another observation that supports this suggestion is the faster oxidation of perillyl alcohol **4a**, which is a primary allylic alcohol, than that of its position isomer **6a**, a secondary allylic alcohol. The Ru–alkoxide intermediates then could undergo a typical β-hydride elimination to give a corresponding carbonyl product and Ru–hydride species. The re-oxidation of the latter by molecular oxygen regenerates Ru–hydroxide species and completes the catalytic cycle.

4. Conclusions

Ruthenium hydroxide supported on silica-coated magnetic nanoparticles is an effective catalyst for the liquid-phase oxidation of a wide range of alcohols using environmentally benign molecular oxygen as a sole oxidant in the absence of any co-catalysts or additives. The oxidation of various biomass-based monoterpenic alcohols can give carbonylic terpenoids, useful for fragrance and pharmaceutical industries, in good to excellent yields. The catalyst is truly heterogeneous; it can be re-covered magnetically and re-used without the significant lost of the catalytic activity and selectivity.

Acknowledgments

The authors would like to express their gratitude to Prof. Pedro K. Kiyohara (IFUSP) for the use of TEM facilities. This research was supported by CNPq, CAPES, FAPESP, FAPEMIG, and INCT-Catálise (Brazil).

References

[1] R.A. Sheldon, I.W.C.E. Arends, A. Dijksman, Catal. Today 57 (2000) 157.
[2] J. Muzart, Tetrahedron 59 (2003) 5789.
[3] M.J. Schultz, M.S. Sigman, Tetrahedron 62 (2006) 8227.
[4] K. Mori, T. Hara, T. Mizugaki, K. Ebitani, K. Kaneda, J. Am. Chem. Soc. 126 (2004) 10657.
[5] T. Mallat, A. Baiker, Chem. Rev. 104 (2004) 3037.
[6] T. Nishimura, N. Kakiuchi, M. Inoue, S. Uemura, Chem. Commun. (2000) 1245.
[7] C. Della Pina, E. Falletta, L. Prati, M. Rossi, Chem. Soc. Rev. 37 (2008) 2077.
[8] G.J. Hutchings, Chem. Commun. (2008) 1148.
[9] A. Corma, H. Garcia, Chem. Soc. Rev. 37 (2008) 2096.
[10] K. Yamaguchi, N. Mizuno, Angew. Chem. Int. Ed. 41 (2002) 4538.
[11] N. Mizuno, K. Yamaguchi, Catal. Today 132 (2008) 18.
[12] K. Yamaguchi, N. Mizuno, Chem. Eur. J. 9 (2003) 4353.
[13] T. Matsushita, K. Ebitani, K. Kaneda, Chem. Commun. (1999) 265.
[14] H.-B. Ji, K. Ebitani, T. Mizugaki, K. Kaneda, Catal. Commun. 3 (2002) 511.
[15] M. Kotani, T. Koike, K. Yamaguchi, N. Mizuno, Green Chem. 8 (2006) 735.
[16] K. Mori, S. Kanai, T. Hara, T. Mizugaki, K. Ebitani, K. Jitsukawa, K. Kaneda, Chem. Mater. 19 (2007) 1249.
[17] S. Venkatesan, A.S. Kumar, J.-F. Lee, T.-S. Chan, J.-M. Zen, Chem. Commun. (2009) 1912.
[18] M.J. Jacinto, O.H.C.F. Santos, R.F. Jardim, R. Landers, L.M. Rossi, Appl. Catal. A 360 (2009) 177.
[19] T. Sato, T. Komanoya, Catal. Commun. 10 (2009) 1095.
[20] K. Yamaguchi, J.W. Kim, J. He, N. Mizuno, J. Catal. 268 (2009) 343.
[21] D.V. Bavykin, A.A. Lapkin, P.K. Plucinski, J.M. Friedrich, J. Catal. 235 (2005) 10.
[22] A. Köckritz, M. Sebek, A. Dittmar, J. Radnik, A. Brückner, U. Bentrup, M.-M. Pohl, H. Hugl, W. Mägerlein, J. Mol. Catal. A 246 (2006) 85.
[23] B.-Z. Zhan, M.A. White, T.-K. Sham, J.A. Pincock, R.J. Doucet, K.V.R. Rao, K.N. Robertson, T.S. Cameron, J. Am. Chem. Soc. 125 (2003) 2195.
[24] H. Yu, X. Fu, C. Zhou, F. Peng, H. Wang, J. Yang, Chem. Commun. (2009) 2408.
[25] V. Polshettiwar, R.S. Varma, Org. Biomol. Chem. 7 (2009) 37–40.
[26] V. Polshettiwar, R.S. Varma, Chem. Eur. J. 15 (2009) 1582–1586.
[27] V. Polshettiwar, B. Baruwati, R.S. Varma, Chem. Commun. (2009) 1837–1839.
[28] S.E. García-Garrido, J. Francos, V. Cadierno, J.-M. Basset, V. Polshettiwar, ChemSusChem 4 (2011) 104–111.
[29] V. Polshettiwar, R. Luque, A. Fihri, H. Zhu, M. Bouhrara, J.-M. Basset, Chem. Rev. 111 (2011) 3036–3075.
[30] L. Menini, M.J. da Silva, M.F.F. Lelis, J.D. Fabris, R.M. Lago, E.V. Gusevskaya, Appl. Catal. A 269 (2004) 117.
[31] L. Menini, M.C. Pereira, L.A. Parreira, J.D. Fabris, E.V. Gusevskaya, J. Catal. 254 (2008) 355.
[32] L. Menini, M.C. Pereira, A.C. Ferreira, J.D. Fabris, E.V. Gusevskaya, Appl. Catal. A 392 (2011) 151.
[33] M.J. Jacinto, P.K. Kiyohara, S.H. Masunaga, R.F. Jardim, L.M. Rossi, Appl. Catal. A 338 (2008) 52.
[34] M.J. Jacinto, R. Landers, L.M. Rossi, Catal. Commun. 10 (2009) 1971.
[35] L.M. Rossi, I.M. Nangoi, N.J.S. Costa, Inorg. Chem. 48 (2009) 4640.
[36] R.L. Oliveira, P.K. Kiyohara, L.M. Rossi, Green Chem. 12 (2010) 144.
[37] C. Sell, in: C. Sell (Ed.), The Chemistry of Fragrances: From Perfumer to Consumer, second ed., vol. 2, RSC Publishing, Dorset, UK, 2006, p. 52.
[38] P.A. Robles-Dutenhefner, K.A. da Silva Rocha, E.M.B. Sousa, E.V. Gusevskaya, J. Catal. 265 (2009) 72.
[39] J.A. Gonçalves, M.J. da Silva, D. Piló-Veloso, O.W. Howarth, E.V. Gusevskaya, J. Organomet. Chem. 690 (2005) 2996.
[40] M.G. Speziali, P.A. Robles-Dutenhefner, E.V. Gusevskaya, Organometallics 26 (2007) 4003.
[41] M.G. Speziali, V.V. Costa, P.A. Robles-Dutenhefner, E.V. Gusevskaya, Organometallics 28 (2009) 3186.
[42] L.A. Parreira, L. Menini, J.C. da Cruz Santos, E.V. Gusevskaya, Adv. Synth. Catal. 352 (2010) 1533.
[43] V. Mazzieria, N. Fıgolia, F.-C. Pascualb, P. L'Argentiere, Catal. Lett. 102 (2005) 79.
[44] H. Yeung, H. Chan, C.G. Takoudis, M.J. Weaver, J. Catal. 172 (1997) 336.
[45] K. Yamaguchi, T. Koike, J.W. Kim, Y. Ogasawara, N. Mizuno, Chem. Eur. J. 14 (2008) 11480.
[46] A. Foelske, O. Barbieri, M. Hahn, R. Kötz, Electrochem. Solid State 9 (2006) A268.
[47] K.A. da Silva, I.V. Kozhevnikov, E.V. Gusevskaya, J. Mol. Catal. 192 (2003) 129.